Inorganic Chemistry

Article

pubs.acs.org/IC

Comparative Thermodynamic Analysis of Zinc Binding to the His/Cys Motif in Virion Infectivity Factor

Sudipa Ghimire-Rijal and Ernest L. Maynard, Jr.*

Department of Biochemistry and Molecular Biology Uniformed Services University of the Health Sciences 4301 Jones Bridge Road, Bethesda, Maryland 20814-4799 United States

Supporting Information

ABSTRACT: HIV-1 virion infectivity factor (Vif) is an accessory protein that induces the proteasomal degradation of the host restriction factor, apolipoprotein B mRNA-editing enzyme catalytic polypeptide-like 3G (APOBEC3G). Degradation of APOBEC3G requires the interaction of Vif with Cul5, the scaffold for an E3 ubiquitin ligase. A highly conserved region in HIV-1 Vif termed the HCCH motif binds zinc and is critical for recruitment of Cul5 and degradation of APOBEC3G. To gain thermodynamic and mechanistic insight into zinc binding to diverse Vif proteins, we have employed a combination of isothermal titration calorimetry, analytical ultracentrifugation, and Cul5 pull down assays. The proton linkage of zinc binding to HIV-1 Vif was analyzed under different buffer conditions and consistent with the release of two Cys-thiol protons upon zinc binding, supporting earlier EXAFS studies. Zinc binding to Vif proteins from HIV-1, SIV_{Agm}, HIV-2, and SIV_{Mac} followed a trend in which the enthalpy of zinc binding became less favorable and the entropy of zinc binding became more favorable. Using AUC, we determined that zinc induced oligomerization of Vif proteins from HIV-1 and SIV_{Agm} but had little or no effect on the oligomeric properties of Vif proteins from HIV-2 and SIV_{Mac}. The zinc dependence of Cul5 recruitment by Vif was investigated. All Vif proteins except HIV-2 Vif required zinc to stabilize the interaction with Cul5. The trends in enthalpy−entropy compensation, zinc-induced oligomerization, and Cul5 recruitment are discussed in terms of the *apo* conformation of the HCCH motif and the role of zinc in stabilizing the structure of Vif.

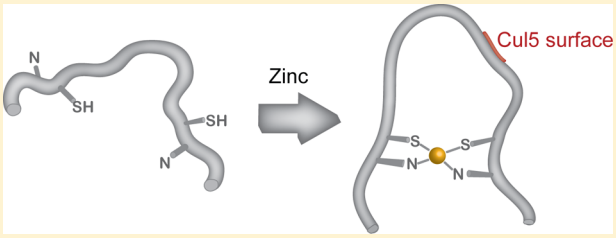

INTRODUCTION

A major role of zinc in biology is to stabilize protein structure. For example, the zinc finger (Cys_2His_2) motif present in transcription factor IIIA[1] binds zinc and adopts a $\beta\beta\alpha$ fold that makes specific contacts within the major groove of DNA.[2−5] Several studies have used the Cys_2His_2 zinc finger as a model to understand the thermodynamics of zinc-coupled protein folding.[6] These studies indicate that the enthalpy of the reaction is dominated by zinc−peptide bond formation, while dehydration of the metal ion makes significant and favorable contributions to the overall reaction entropy. However, enthalpy−entropy compensation (EEC) for the zinc-induced folding of small domains like the zinc finger involves many factors and is extremely dependent on the system.[7] Most studies to date have employed zinc finger peptides (25 amino acids on average) derived from DNA-binding transcription factors. Relatively less is known about the interplay of enthalpy and entropy of the zinc-induced folding of larger domains that mediate protein−protein interactions.

Zinc is essential for the function of the HIV-1 accessory protein, virion infectivity factor (Vif). Vif is required for HIV-1 replication in CD4-positive T cells, which express members of the apolipoprotein B mRNA editing catalytic polypeptide (APOBEC) family of cytidine deaminases. Certain members of this enzyme family (e.g., APOBEC3G) deaminate cytidines in viral reverse transcripts, and thus pose an innate barrier to viral replication.[8] Vif functions as an adaptor protein that recruits a cullin-5 (Cul5) based ubiquitin ligase to induce the polyubiquitination and proteasomal degradation of APOBEC3G.[9−14] Zinc binds reversibly to the conserved HCCH motif (**His**-X_5-**Cys**-X_{17-18}-**Cys**-X_{3-5}-**His**) in HIV-1 Vif.[15] High-resolution structures of this region are not available, but EXAFS experiments using a peptide encompassing the HCCH motif (residues 101−142 of HIV-1 Vif) are consistent with tetrahedral N_2S_2 coordination of zinc.[16] This HCCH peptide binds directly to Cul5 in a zinc-dependent manner,[16] suggesting that zinc stabilizes a biologically active conformation of Vif. Consistent with this, circular dichroism spectroscopy reveals significant changes in HCCH motif secondary structure that are induced by zinc binding and reversed by the addition of EDTA.[15]

The HCCH motif is conserved in Vif proteins from HIV-1, HIV-2, SIV_{Agm} (African green monkey), and SIV_{Mac} (rhesus macaque) (Figure 1), suggesting a common zinc-dependent mode of interaction with the host Cul5. Despite the high degree of conservation of the His and Cys ligands, there are still significant differences in the intervening sequences that may affect metal binding or protein folding. In this paper, we have used isothermal titration calorimetry (ITC) and analytical

Received: November 22, 2013
Published: April 16, 2014

   dx.doi.org/10.1021/ic402907g | *Inorg. Chem.* 2014, 53, 4295−4302

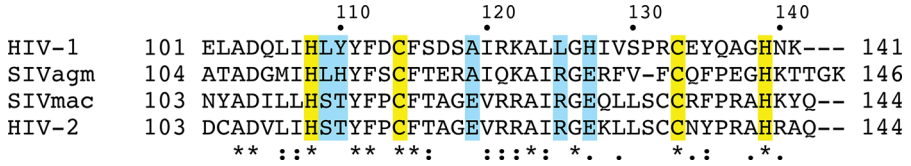

Figure 1. ClustalW sequence alignment of the HCCH region of Vif proteins encoded by HIV-1, HIV-2, SIV_{Agm}, and SIV_{Mac}. Numbering on the top of the sequences corresponds to the amino acid numbering for HIV-1 Vif. Amino acids that constitute the HCCH motif are highlighted in yellow. Amino acids highlighted in light blue are highly or absolutely conserved in each family of Vif sequences, but have different polar/apolar properties.

ultracentrifugation (AUC) to characterize metal binding to the HCCH motifs of Vif proteins from HIV-1, HIV-2, SIV_{Mac}, and SIV_{Agm}.

Here, we report that the HCCH motifs of diverse Vif proteins employ varying degrees of EEC to achieve similar zinc binding affinity. The proton linkage of zinc binding to HIV-1 Vif was analyzed under different buffer conditions and was consistent with the release of two Cys-thiol protons, as expected for zinc coordination by the two conserved Cys residues in the HCCH motif. As we discuss, the observed variation in EEC could indicate differences in metal ion coordination or could reflect differences in protein conformation. AUC experiments revealed varying effects of zinc on the oligomeric state of Vif, and we found that zinc stabilized the interaction between Vif and Cul5 to widely varying degrees. Together, these findings further support the idea that evolutionary variation in Vif sequence has produced significant differences in *apo*- and zinc-bound protein conformations. Although further work is required to elucidate the differences in zinc binding-site structure for these Vif proteins, this study suggests that the importance of zinc in stabilizing the Vif-Cul5 interaction may not be universal.

EXPERIMENTAL SECTION

Cloning, Protein Expression, and Purification. DNA vectors encoding Vif from HIV-1 (HXB2), HIV-2, SIV_{Agm}, and SIV_{Mac} were kind gifts from Klaus Strebel (NIAID/NIH). HCCH constructs were designed based on alignment with residues 101−141 of HIV-1 Vif (Figure 1). DNA fragments encoding residues 101−141 of HIV-1 Vif, residues 103−144 of HIV-2 Vif, residues 104−146 of SIV_{Agm} Vif, and residues 103−144 of SIV_{Mac} Vif were amplified by PCR and cloned into the *Eco*RI-*Sbf*I site of a variant of the pMal c-5x vector (NEB) in order to produce fusions to maltose binding protein (MBP). Sequence-confirmed constructs were transformed into BL21 (DE3) *Escherichia coli* and cultures were maintained in 2YT broth containing ampicillin and 1% glucose at 37 °C until OD_{600} reached 0.5. Protein expression was induced with 0.5 mM IPTG and allowed to occur for 16 h at 18 °C. Cells were harvested by centrifugation at 5500 × *g* and 4 °C for 10 min and stored at −80 °C.

Cell pellets were resuspended (1g in 10 mL buffer) in 20 mM HEPES pH 7.5, 150 mM NaCl, 200 μM TCEP, supplemented with RNase/DNase (Pierce) and protease inhibitor (Roche Applied Sciences), and lysed using a French pressure cell. Lysates were clarified by centrifugation at 18 000 × *g* and 4 °C for 50 min. The supernatant was filtered (0.45 μm PVDF) and incubated with amylose resin (NEB) for 1 h at 4 °C with gentle rocking. The resin was washed with 10 column volumes of resuspension buffer, followed by 5 column volumes of buffer containing 20 mM HEPES pH 8.0, 20 mM NaCl, and 200 μM TCEP. Proteins were eluted using 30 mL of the same buffer containing 10 mM maltose and were ∼90% pure according to SDS-PAGE analysis. Proteins were loaded onto a Resource Q column (GE Healthcare) and after washing were eluted with a linear gradient from 20 mM NaCl to 1 M NaCl over 10 column volumes. MBP-Vif proteins were further purified using a Superose 6 column (GE Healthcare) equilibrated in buffer containing 20 mM HEPES pH 7.5, 150 mM NaCl, and 200 μM TCEP and operated at a flow rate of 0.5 mL min^{-1}. Protein concentration was determined by either Bradford assay (Bio-Rad) using bovine serum albumin as a standard or by the method of Edelhoch as described in Pace et al.[17]

Isothermal Titration Calorimetry. ITC experiments were performed at 25 °C using a MicroCal iTC200 microcalorimeter (GE Healthcare). $Zn(NO_3)_2$ was diluted from a standardized stock solution (Sigma) into the appropriate titration buffer (see text for details). This solution was loaded in the ITC syringe and injected into the cell, which contained a solution of purified maltose binding protein-Vif (MBP-Vif) fusion in the same buffer stirred at 1000 rpm. Under these conditions, HIV-1 Vif (40 μM) and HIV-2 Vif (40 μM) were titrated with 730 μM $Zn(NO_3)_2$ while SIV_{Agm} Vif (80 μM) and SIV_{Mac} Vif (80 μM) were titrated with 1.0 mM $Zn(NO_3)_2$. After the first injection of 0.4 μL $Zn(NO_3)_2$ into the cell, 19 additional 2-μL injections were made into the cell with 2 min between injections to allow the system to return to equilibrium (baseline).

ITC titrations were performed 2−3 times for each type of experiment to ensure consistency. To control for dilution and metal−buffer effects, zinc was titrated into buffer or into buffer containing an equivalent concentration of purified MBP; both titrations gave identical results. All ITC data were corrected by subtracting the heats from the zinc-into-buffer control titration from the experimental titration data. ITC data are presented as the background-corrected titration (heat flow in μcal/s versus time) in the top panel and the peak-integrated molar heat per aliquot (kcal per mol of injectant) versus the molar ratio of zinc-to-Vif in the bottom panel. Solid lines in the bottom panel reflect the best fit to the data using the single-site binding model in the MicroCal Origin software package. Thermodynamic parameters presented in table form are the best-fit results from global analysis of replicate ITC titration data using the single-site model in the program SEDPHAT.[18] Results from SEDPHAT global analysis of the integrated ITC data were essentially identical to those obtained when the data were analyzed individually in MicroCal Origin. In determining the proton linkage of zinc binding, standard ionization enthalpies for MES[19] and [HEPES, Bis-Tris, and Tris-HCl][20] were used.

Analytical Ultracentrifugation. Sedimentation velocity experiments were conducted at 20.0 °C on a Beckman Coulter Proteome XL-A analytical ultracentrifuge using the absorbance optical detection system. Samples (35 μM for all MBP-Vif/HCCH constructs) were loaded into 2-channel, 12 mm path length sector shaped cells (400 μL). Scans were acquired at 4 min intervals and rotor speeds of 45 000 rpm; absorbance data were collected as single absorbance measurements at either 280 or 250 nm using a radial spacing of 0.003 cm.

Data were analyzed in SEDFIT 11.9b[21] in terms of a continuous $c(s)$ distribution. Solution densities ρ and viscosities η were calculated using the program SEDNTERP 1.2,[22] as were values for the partial specific volume v of the protein. The $c(s)$ analyses were carried out using an s range of 0 to 25 with a linear resolution of 200 and maximum entropy regularization confidence levels (F-ratio) of 0.68. In all cases, excellent fits were observed with root-mean-square deviations ranging from 0.0030−0.0091 absorbance units. Sedimentation coefficients were corrected to standard conditions at 20.0 °C in water, $s_{20,w}$. $C(s)$ were plotted after normalization using the program GUSSI (kindly provided by Chad Brautigam, UT Southwestern Medical Center).

Vif−Cul5 Pulldown Assay. Purified MBP-Vif and Cul5(1−384) proteins were treated with Chelex resin (Biorad) to remove any bound metal ions, following the manufacturer's suggested protocol. Amylose

dx.doi.org/10.1021/ic402907g | *Inorg. Chem.* 2014, 53, 4295−4302

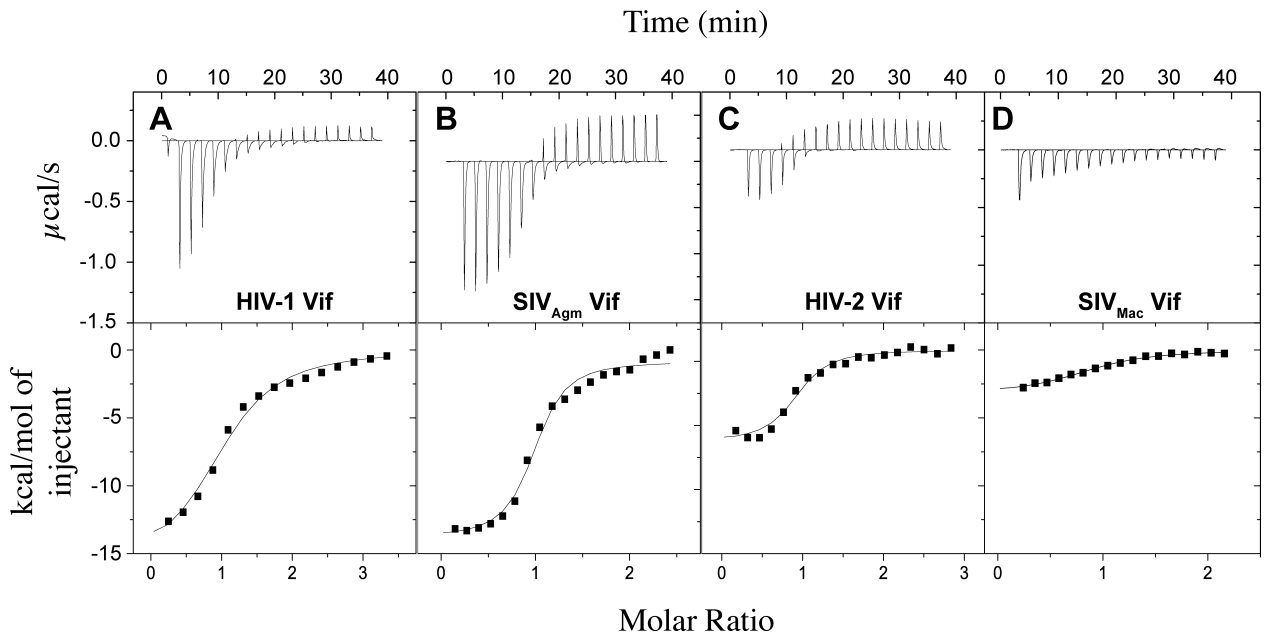

Figure 2. Isothermal titration calorimetry data for zinc titrations into (A) HIV-1 Vif, (B) SIV$_{Agm}$ Vif, (C) HIV-2 Vif, and (D) SIV$_{Mac}$ Vif constructs. For comparison, raw thermogram data (top panels) and integrated data (bottom panels) are displayed using the same scale.

Table 1. Thermodynamic Parameters from Calorimetric Analysis of Zinc Binding to Vif at 298 K[a]

protein	stoichiometry (n)	K_d (μM)	$\Delta G°$ (kcal/mol)	$\Delta H°$ (kcal/mol)	$-T\Delta S°$ (kcal/mol)
HIV-1 Vif	1.0 ± 0.1	4.5 ± 0.1	−7.3 ± 0.2	−15.7 ± 0.4	+8.4 ± 0.4
SIV$_{Agm}$ Vif	1.1 ± 0.2	2.5 ± 0.3	−7.6 ± 0.9	−15.6 ± 0.2	+8.0 ± 0.5
HIV-2 Vif	1.0 ± 0.2	3.8 ± 0.4	−7.4 ± 0.8	−8.2 ± 0.2	+0.8 ± 0.4
SIV$_{Mac}$ Vif	1.0 ± 0.2	11.5 ± 0.4	−6.7 ± 0.2	−3.0 ± 0.2	−3.7 ± 0.3

[a]Values of n, K_d, and $\Delta H°$ were determined from fitting a single-binding-site model to 2−3 data replicates (Supporting Information). $\Delta G°$ was calculated from the equation $\Delta G° = -RT \ln K_{eq}$. Error in $\Delta G°$ was calculated from the fractional error associated with K_d. Error in $T\Delta S°$ was calculated as the quadratic sum of errors in $\Delta G°$ and $\Delta H°$.

resin (250 μL packed bed volume) was incubated with 2 mg MBP-Vif in buffer containing 20 mM HEPES pH 7.5, 150 mM NaCl, and 200 μM TCEP for 30 min at 4 °C. Buffer and unbound protein was removed by centrifugation and the resin was washed 4 times with 1 mL aliquots of the same buffer. Cul5 (2 mg) was added to the resin and incubated for 20−30 min on ice in the absence or presence of zinc (1 mol equiv relative to MBP-Vif). Unbound protein was removed by centrifugation and the resin was washed 5 times with 1 mL aliquots of buffer. Finally, 40 μL of 40 mM maltose was added to the resin and after 10 min, proteins in the supernatant were separated by SDS-PAGE and visualized by staining with Colloidal Blue (Invitrogen). Cul5 band intensities were quantified using ImageJ software (NIH) and normalized for variations in the amount of MBP-Vif.

RESULTS

Zinc Binding to Vif Proteins Encoded by HIV-1, HIV-2, SIV$_{Mac}$, and SIV$_{Agm}$. The HCCH motifs of Vif proteins from HIV-1, HIV-2, SIV$_{Mac}$, and SIV$_{Agm}$ are highly conserved (Figure 1). Vif HCCH constructs were designed based on residues 101−141 in HIV-1 Vif and isothermal titration calorimetry (ITC) was used to compare the thermodynamics of zinc binding. Vif constructs were expressed from the pMal-c5X vector and purified as described in the Experimental Section. Proteins were concentrated in 20 mM HEPES pH 7.4, 150 mM NaCl, 200 μM TCEP, loaded into the cell of the ITC, and titrated with $Zn(NO_3)_2$ prepared in the same buffer (Experimental Section). The titration data are shown in Figure 2. The raw thermogram data indicate that in all cases zinc binding was exothermic. However, endothermic peaks became apparent when the molar ratio of zinc increased beyond 1. The endothermic peaks were most pronounced for zinc titrations of HIV-2 Vif, SIV$_{Agm}$ Vif, and HIV-1 Vif (Figure 2, panels A-C). The endothermic peaks may be related to oligomerization, which has been well characterized for HIV-1 Vif.[23−26] Zinc induced oligomerization was also observed for these proteins in AUC experiments, which are presented later. Endothermic peaks could also result from nonspecific binding of zinc to the proteins (discussed below).

After subtraction of buffer background (heats of zinc dilution into buffer), the injection peaks were integrated, and a single-site binding model was fitted to the data (Figure 2, bottom panels) as described in the Experimental Section. The best-fit thermodynamic parameters are presented in Table 1. Errors shown are the result of global analysis of two to three replicate data sets (Supporting Information Table 1). The analysis indicates that the data are generally in good agreement with the single-site model. The affinities of zinc binding were all in the low μM range, although the affinity of zinc binding to SIV$_{Mac}$ Vif (K_d = 11.5 μM) was significantly lower than to the other Vif proteins ($K_d \approx 2-5$ μM). The best-fit curves for zinc titration of HIV-1 Vif, SIV$_{Agm}$ Vif, and HIV-2 Vif (bottom panels A−C of Figure 2) deviated in the early data points, suggesting that a binding model incorporating a second low-affinity site might provide a better fit. The ITC data were analyzed using the sequential binding model in Origin. The fit to the titration data

dx.doi.org/10.1021/ic402907g | Inorg. Chem. 2014, 53, 4295−4302

for HIV-1 Vif produced a smaller K_d (0.9 ± 0.2 μM) compared to the K_d derived from the single-site model (4.5 μM). The K_d values for the other Vif proteins were slightly weaker than or within error of the values from the single-site model (Supporting Information Table 2). The sequential binding model generally produced smaller values of ΔH for HIV-1, SIV_{Agm}, and HIV-2 Vif, while the ΔH value for SIV_{Mac} Vif was within experimental error of the value from the single-site fit. The trends in ΔH for the different Vif proteins remained the same. However, the errors associated with the thermodynamic parameters for the second site were unacceptably large, casting doubt on whether the sequential binding model can provide a realistic description of zinc binding to Vif. For subsequent discussion, we will refer to the best-fit thermodynamic values from the single-site model (Table 1).

The affinity of zinc binding could be considered low. However, zinc binding under physiological conditions may be influenced by the folding of full length Vif and by interactions with cellular factors (e.g., Cul5). In a previous study, we discovered that the interaction of Vif and Cul5 required stoichiometric zinc,[16] a result that suggests coupling of zinc binding, Vif folding, and Cul5 recognition.

HIV-1 Vif and SIV_{Agm} Vif exhibited larger binding enthalpy values ($\Delta H^\circ \approx -16$ kcal/mol), while smaller values were observed for HIV-2 Vif ($\Delta H^\circ = -8.2$ kcal/mol) and SIV_{Mac} Vif ($\Delta H^\circ = -3.0$ kcal/mol). These enthalpy values have not been adjusted for buffer protonation effects. Our comparison is made with the assumption that the Vif proteins undergo the same proton loss during zinc binding. All of the Vif constructs contain two His and two Cys residues that constitute the HCCH motif and are assumed to coordinate zinc similar to the His/Cys coordination proposed for HIV-1 Vif.[16] However, the HCCH motifs of HIV-2 Vif and SIV_{Mac} Vif contain an additional Cys residue adjacent to the second Cys residue in the motif (Figure 1). Whether these adjacent Cys residues play any direct role in metal binding is unknown, although this seems unlikely since Cys is not absolutely conserved at this position in HIV-2 Vif or SIV_{Mac} Vif sequences. The Cys residues are expected to be largely protonated at pH 7.5. Deprotonation of Cys residues upon binding to zinc can constitute a significant fraction of the reaction enthalpy.[27,28]

Similar reaction entropy values were observed for HIV-1 Vif ($-T\Delta S^\circ = +8.4$ kcal/mol) and SIV_{Agm} Vif ($-T\Delta S^\circ = +8.0$ kcal/mol). This could suggest that these proteins undergo a significant conformational change as they bind zinc. The entropic penalty was far less for HIV-2 Vif ($-T\Delta S^\circ = +0.8$ kcal/mol) suggesting that either less conformational reorganization of the HCCH motif is required or release of waters (desolvation) contributes significantly to zinc binding. Zinc binding to the HCCH motif of SIV_{Mac} Vif was entropically favorable ($-T\Delta S^\circ = -3.7$ kcal/mol), presumably because of minimal conformational reorganization and the release of waters of solvation.

The binding of zinc to the HCCH motif in HIV-1 Vif is expected to require deprotonation of the coordinating His and Cys ligands. Since the protons released in such a reaction are taken up by the basic component of the buffer, one can determine the extent of proton linkage by performing titrations in buffers with different heats of ionization.[29] The overall zinc binding reaction is the sum of several subreactions that include dissociation of zinc-buffer complexes (eq 1), release of protons from Vif (eq 2), protonation of the buffer (eq 3), and formation of the Vif–zinc complex (eq 4).

$$\text{buffer—}Zn^{2+} \rightleftarrows Zn^{2+} + \text{buffer} \quad (1)$$

$$\text{Vif—}H^{+} \rightleftarrows \text{Vif} + H^{+} \quad (2)$$

$$\text{buffer} + H^{+} \rightleftarrows \text{buffer—}H^{+} \quad (3)$$

$$Zn^{2+} + \text{Vif} \rightleftarrows \text{Vif—}Zn^{2+} \quad (4)$$

$$\text{buffer—}Zn^{2+} + \text{Vif—}H^{+} \rightleftarrows \text{Vif—}Zn^{2+} + \text{buffer—}H^{+} \quad (5)$$

In accordance with Hess's law the overall reaction enthalpy (ΔH_{rxn}) is

$$\Delta H_{\text{Vif—}Zn^{2+}} + n\Delta H_{\text{buffer—}H^{+}} - \Delta H_{\text{buffer—}Zn^{2+}} - n\Delta H_{\text{Vif—}H^{+}} \quad (6)$$

A plot of the overall reaction enthalpy, corrected for the enthalpy of buffer-metal complex formation ($\Delta H_{rxn} + \Delta H_{buffer-Zn^{2+}}$), versus the buffer protonation enthalpy ($\Delta H_{buffer-H^{+}}$) will yield a line with slope equal to n, the number of protons released during the reaction, and a y-intercept that is the buffer-independent reaction enthalpy ($\Delta H_{Vif-Zn^{2+}} - n\Delta H_{Vif-H^{+}}$).[30]

The buffer dependence of zinc binding to HIV-1 Vif was analyzed under conditions of 20 mM buffer (MES, HEPES, Bis-Tris, or Tris-HCl), 150 mM NaCl, and 200 μM TCEP, adjusted to pH 7.5. A plot of $\Delta H_{rxn} + \Delta H_{buffer-Zn^{2+}}$ against $\Delta H_{buffer-H^{+}}$ is shown in Figure 3. Linear regression analysis gave

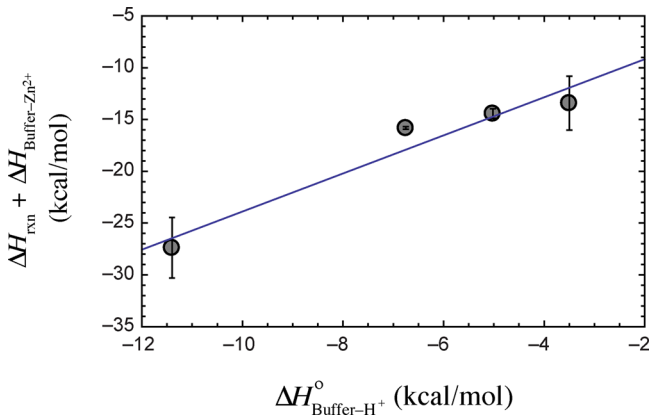

Figure 3. Buffer dependence of the enthalpy of zinc binding to HIV-1 Vif. The overall reaction enthalpy (ΔH_{rxn}) was determined in different buffers (MES, HEPES, Bis-Tris, or Tris-HCl, all adjusted to pH 7.5), and corrected for heats of zinc-buffer complex formation ($\Delta H_{buffer-Zn^{2+}}$). The following values for zinc–buffer complex formation were used: $\Delta H_{MES-Zn^{2+}} = -0.3$ kcal/mol, $\Delta H_{HEPES-Zn^{2+}} = -0.29$ kcal/mol, $\Delta H_{BisTris-Zn^{2+}} = -0.3$ kcal/mol, $\Delta H_{Tris-Zn^{2+}} = -2.45$ kcal/mol.[7,30] Corrected reaction enthalpy ($\Delta H_{rxn} + \Delta H_{buffer-Zn^{2+}}$) is plotted as a function of the enthalpy of buffer ionization ($\Delta H_{buffer-H^{+}}$). Linear regression analysis gave a slope of 1.84 ± 0.33, y-intercept of −5.5 ± 2.4 kcal/mol, and $R^2 = 0.941$.

a slope (n) of 1.84 ± 0.33 and a y-intercept of −5.5 ± 2.4 kcal/mol ($R^2 = 0.941$). Assuming typical pK_a values for histidine (6.5) and cysteine (8.3), a Henderson–Hasselbalch analysis predicts that 1.9 protons would be displaced by zinc binding to Vif at pH 7.5. This value is in good agreement with the n value of 1.84 derived from our analysis. The y-intercept in Figure 3 of −5.5 ± 2.4 kcal/mol reflects the buffer-independent reaction enthalpy and is expressed as $\Delta H_{Vif-Zn^{2+}} - n\Delta H_{Vif-H^{+}}$. The term $n\Delta H_{Vif-H^{+}}$ corresponds to the protonation enthalpy of Vif and the term $\Delta H_{Vif-Zn^{2+}}$ contains all other buffer-independent

dx.doi.org/10.1021/ic402907g | Inorg. Chem. 2014, 53, 4295–4302

enthalpic contributions to the reaction, such as breaking 6 Zn^{2+}−OH_2 bonds, forming Zn^{2+}−S and Zn^{2+}−N coordinate bonds, desolvating the protein, and folding the protein. Therefore, the net enthalpy associated with these processes can be calculated by subtracting the change in enthalpy for His/Cys deprotonation ($-n\Delta H_{Vif-H^+}$) from the buffer-independent reaction enthalpy. Using previously determined ΔH values for deprotonation of His[31] and Cys,[32] we calculate the enthalpy of His/Cys deprotonation at pH 7.5 to be 0.18 His(+8.7 kcal/mol) + 1.72 Cys(+8.5 kcal/mol) = +16.2 kcal/mol. Then the value of $\Delta H_{Vif-Zn^{2+}}$ is (−5.5 ± 2.4) + (−16.2) = −21.7 kcal/mol. As mentioned above, this value also includes contributions from zinc desolvation, protein desolvation, and protein folding. Dissection of the thermodynamics of these processes is very difficult and beyond the scope of this study. However, the value of −21.7 kcal/mol for Vif is very close to the ΔH value of −26.1 kcal/mol reported for CP-1.[27]

The ability of zinc to drive aggregation of Vif may be the result of the exposure of a hydrophobic surface.[15] In support of this hypothesis, Cul5 effectively blocked zinc induced oligomerization of Vif[16] suggesting that a hydrophobic surface is buried and stabilized by the Vif-Cul5 complex. Analytical ultracentrifugation was used to determine the effects of zinc on the oligomeric state of the Vif/HCCH constructs from HIV-1, HIV-2, SIV_{Agm} and SIV_{Mac}. Each construct (35 μM) was prepared in the absence of zinc and analyzed by sedimentation velocity AUC. At the end of the experiment, the AUC cell was opened, 1 mol equiv of zinc was added, and the experiment was repeated. AUC data were analyzed using SEDFIT and normalized according to maximum $c(s)$ value (Experimental Section). The results from this analysis are presented in Figure 4. The HIV-1 Vif data (Figure 4, bottom panel) reveal mostly monomeric species in the absence of added zinc (solid line). Addition of zinc caused a dramatic increase in the amount of dimeric and higher-order oligomeric species (dashed line). Previous studies using circular dichroism spectroscopy[15] and AUC[24] have established that aggregation caused by zinc binding to the HCCH motif is readily reversed by the addition of EDTA. SIV_{Agm} Vif, like HIV-1 Vif, formed primarily monomeric species with a trace of dimeric species and some higher-order species observed in the absence of zinc. Zinc caused dimeric species to increase by an amount that nearly matched HIV-1 Vif, but did not increase the amount of higher-order oligomeric species. In the absence of zinc, HIV-2 Vif was mostly monomeric with a slightly elevated level of dimeric species compared to HIV-1 Vif and SIV_{Agm} Vif. Zinc increased the amount of dimeric species, but did not lead to the formation of higher-order oligomeric species. SIV_{Mac} Vif was unique in that its oligomeric profile was unaffected by the addition of zinc and consisted of almost entirely monomeric species with a trace of dimeric species. This is similar to the behavior in the ITC thermograms (see Figure 2), where endothermic peaks were observed during the zinc titration of HIV-1 Vif (Figure 2A), SIV_{Agm} Vif (Figure 2B), HIV-2 Vif (Figure 2C), but not for SIV_{Mac} Vif (Figure 2D).

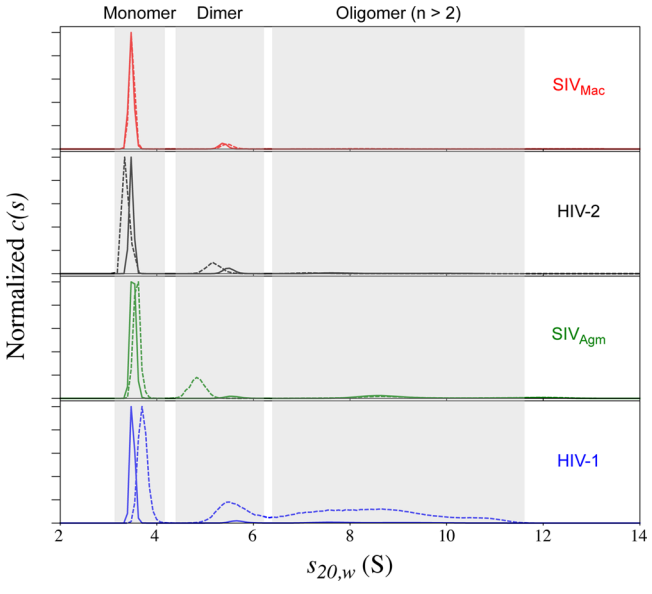

Figure 4. Sedimentation velocity analytical ultracentrifugation of HIV-1, HIV-2, SIV_{Mac}, and SIV_{Agm} Vif constructs (35 μM loading concentration) in the absence (solid lines) and presence (dashed lines) of zinc. Data were analyzed as a continuous $c(s)$ distribution in SEDFIT as described in the Experimental Section.

We previously reported that a direct and zinc-dependent interaction is formed between HIV-1 Vif and human Cul5.[16] We wanted to determine whether the zinc-dependent interaction between HIV-1 Vif and Cul5 is a property that is conserved for other retroviral Vif proteins. Given that Cul5 sequences from human and nonhuman primates are identical in their cullin-repeat domains we used purified human Cul5(1−384) which contains the entire cullin domain. MBP-Vif constructs were treated with Chelex resin, immobilized on amylose resin, and used to pull down human Cul5(1−384) (Experimental Section). The results are shown in Figure 5. The

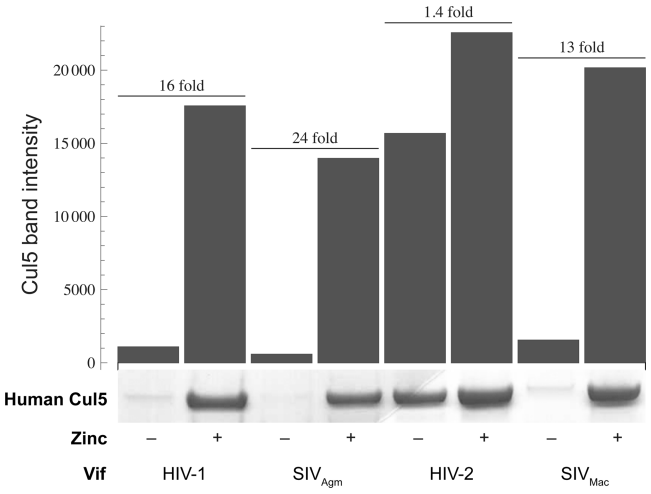

Figure 5. Pull down of human Cul5 by MBP-Vif constructs. Equal amounts of each construct was loaded onto amylose resin and incubated with Cul5 in the absence or presence of a stoichiometric amount of zinc (Experimental Section). Raw band intensities (obtained from densitometric analysis with ImageJ software) are plotted and fold increase in Cul5 binding in the presence of zinc is indicated for each construct.

interaction between HIV-1 Vif and Cul5 required zinc, which increased the amount of Cul5 pulled down by 16-fold, a result that is consistent with our earlier report that the amount of Vif pulled down by Cul5(1−384) increases in the presence of stoichiometric zinc.[16] Vif proteins from SIV_{Agm} and SIV_{Mac} also recruited Cul5 in a zinc-dependent manner, with the amount of Cul5 pulled down increasing by 24 fold for SIV_{Agm} Vif and 13-

dx.doi.org/10.1021/ic402907g | Inorg. Chem. 2014, 53, 4295−4302

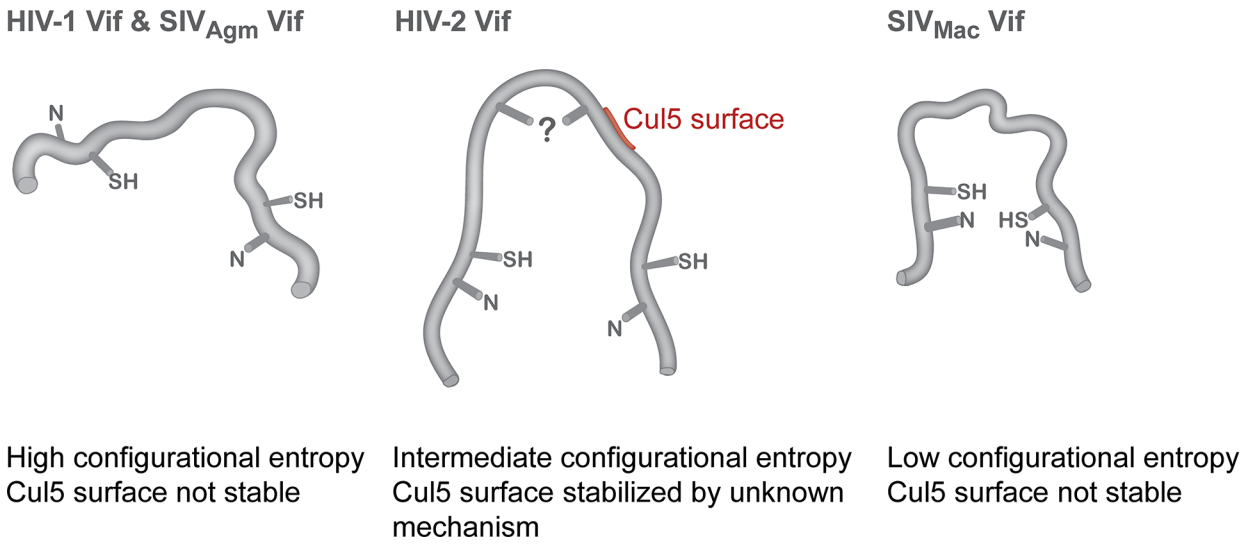

Figure 6. Model to explain zinc binding and Cul5 recognition by Vif proteins. His and Cys ligands from the HCCH motif are represented as N or SH, respectively.

fold for SIV_{Mac} Vif. In the absence of added zinc, Vif proteins from HIV-1, SIV_{Agm}, and SIV_{Mac} did not pull down a significant amount of Cul5. HIV-2 Vif exhibited different behavior. In the absence of zinc, the amount of Cul5 pulled down by HIV-2 Vif was comparable to that pulled down by the other Vif proteins in the presence of zinc. Furthermore, the amount of Cul5 pulled down by HIV-2 Vif in the presence of zinc increased only 1.4 fold (Figure 5).

DISCUSSION

The enthalpy−entropy compensation (EEC) of zinc binding to the Vif/HCCH motifs under investigation follows a pattern (HIV-1 → SIV_{Agm} → HIV-2 → SIV_{Mac}) in which binding enthalpy (ΔH°) becomes less favorable and binding entropy ($-T\Delta S^\circ$) becomes increasingly more favorable (Table 1). The extremes in this pattern, represented by the HCCH motifs of HIV-1 Vif and SIV_{Mac} Vif, suggest differences in the mode of zinc binding, and could arise from changes in zinc coordination or from peptide conformational differences. HIV-1 Vif and SIV_{Agm} Vif each contain 2 Cys residues, while SIV_{Mac} Vif and HIV-2 Vif contain 3 and 4 Cys residues, respectively. However, since the Cys and His residues that constitute the HCCH motif are absolutely conserved (Figure 1), it is reasonable to assume that the Vif proteins from SIV_{Agm}, HIV-2, and SIV_{Mac} coordinate zinc using the same Cys_2His_2 coordination employed by HIV-1 Vif.[16] We favor this model and propose that the *apo*-Vif conformation is the major feature that differs between the HCCH motifs and contributes to the observed EEC. We also discuss the possibility that the observed trend in EEC could arise from a change in the zinc coordination motif.

To discuss the observed trends in EEC, it is important to note that the reaction enthalpy values in Table 1 are dependent on the buffer. Assuming all Vif proteins under investigation release the same number of protons on zinc binding, a trend is observed in which ΔH is similar for HIV-1 Vif and SIV_{Agm} Vif, but becomes increasingly less favorable for HIV-2 Vif and SIV_{Mac} Vif. Conversely, $T\Delta S$ is similar for HIV-1 Vif and SIV_{Agm} and becomes increasingly more favorable for HIV-2 Vif and SIV_{Mac} Vif. This is consistent with a higher degree of configurational entropy for HIV-1 Vif and SIV_{Agm} Vif and a lower entropic penalty for HIV-2 Vif and SIV_{Mac} Vif (Figure 6).

Another possible explanation is that Vif proteins from HIV-2 Vif and SIV_{Mac} Vif utilize a different coordination motif to bind zinc. Similar EEC trends have been found other systems that contain increasing numbers of zinc-coordinating Cys thiols and have been attributed to Cys-thiol deprotonation.[7,28] If HIV-2 Vif and SIV_{Mac} have a greater number of coordinating Cys residues, the changes in reaction enthalpy could be explained by a correspondingly larger buffer protonation enthalpy.

The folding of zinc fingers is thermodynamically coupled to zinc binding (eqs 7−9). Therefore, the observed free energy of metal binding ($\Delta G_{ML\text{-observed}}$) is less than the true metal binding free energy (ΔG_{ML}) by the energetic cost of protein folding ($\Delta G_{apo\text{-folding}}$) as described by Reddi et al.[28]

protein folding

$$L_U \rightleftharpoons L_F \quad \Delta G_{apo\text{-folding}} \tag{7}$$

metal ligation

$$L_F + M \rightleftharpoons L_F - M \quad \Delta G_{ML} \tag{8}$$

overall reaction

$$L_U + M \rightleftharpoons L_F - M \quad \Delta G_{ML\text{-observed}} \tag{9}$$

Estimates for $\Delta G_{apo\text{-folding}}$ vary greatly and are highly dependent on the experimental system. Blasie and Berg performed structure-based thermodynamic analysis of the zinc finger consensus peptide 1 (CP-1) and estimated $\Delta G_{apo\text{-folding}}$ to be +17 kcal/mol.[27] Reddi et al. determined $\Delta G_{apo\text{-folding}}$ using unstructured peptide scaffolds for which the energetic difference between *apo*-folded and *apo*-unfolded states (L_F and L_U, respectively) is very close to zero, which allowed the authors to determine ΔG_{ML} for different coordination types (since $\Delta G_{ML\text{-observed}} \approx \Delta G_{ML}$). On the basis of comparison of $\Delta G_{ML\text{-observed}}$ for C_2H_2 peptide scaffolds and C_2H_2 zinc finger proteins, $\Delta G_{apo\text{-folding}}$ was found to fall in the range of 0 to +6 kcal/mol.[28] The values of $\Delta G_{ML\text{-observed}}$ listed in Table 1 cluster around −7.3 kcal/mol. If we use the value ΔG_{ML} = −16.5 kcal/mol determined for metal ligation by the C_2H_2 peptide scaffold,[28] we calculate that $\Delta G_{apo\text{-folding}}$ for Vif is −7.3 − (−16.5) = +9.2 kcal/mol. This value is less than calculated for CP-1 and larger than the values calculated for C_2H_2 zinc fingers

dx.doi.org/10.1021/ic402907g | *Inorg. Chem.* 2014, 53, 4295−4302

by Reddi et al. and is the amount of free energy derived from metal binding that is used to drive folding of the HCCH domain in Vif.

The energetic penalty for folding the HCCH domain (+9.2 kcal/mol) is more than 50% of the free energy of zinc ligation (−16.5 kcal/mol) reported for the C_2H_2 peptide scaffold.[28] This is in contrast to the other C_2H_2 zinc fingers analyzed by Reddi et al.[28] where only 10−20% of the metal ligation free energy is used to offset the folding penalty. One important characteristic of the HCCH domain in HIV-1 Vif is that the *apo*-state is not unstructured as is the case for most zinc fingers. Far-UV circular dichroism studies of a HCCH peptide (HIV-1 Vif residues 101−142) indicate that the *apo*-state exists in a conformation with 12% α helix, 33% beta-sheet, and 55% random coil.[16,33] The existence of tertiary structure in the *apo*-state is supported by near-UV CD spectra and intrinsic tryptophan fluorescence spectra of the HCCH peptide.[33] The larger $\Delta G_{\text{apo-folding}}$ value could be explained if zinc-induced folding of Vif requires disruption of the *apo*-conformation of the HCCH domain.

The enthalpy of protein folding is largely determined by changes in accessible polar and apolar surface area.[36,37] However, if the *apo* forms of HIV-2 Vif and SIV_{Mac} Vif are partially structured, zinc binding may have less of an effect on overall folding, and changes in polar and apolar surface area would provide less of a driving force. The enthalpy of zinc binding could become less favorable due to charge effects of on the pK_a of the coordinating His/Cys ligands. For example, desolvation of an ionizable group often perturbs the pK_a value in such a way that reflects the greater stability of the neutral form over the charged species.[38] For example, if the Cys-SH ligands in the HCCH motif are more buried in SIV_{Mac} Vif, their pK_a values could be elevated, making them more difficult to deprotonate and stabilizing the thiol form. Dipole and charge effects (attraction or repulsion) can also perturb the pK_a of an ionizable group.[38] It is worth noting that the HCCH sequences from SIV_{Mac} Vif and HIV-2 Vif each contain an additional Cys residue adjacent to the putative metal-binding Cys residue (Figure 1). Thus, dipole or charge interactions could result in a higher Cys-SH pK_a and affect the enthalpy of deprotonation. Although many questions still exist, our data provide the groundwork for future studies to obtain a more complete picture of the folding energetics of Vif.

The HCCH motifs of HIV-1 Vif and SIV_{Agm} Vif oligomerized in the presence of stoichiometric zinc, while the HCCH motifs belonging to HIV-2 Vif and SIV_{Mac} Vif did not (Figure 4). Zinc-induced oligomerization of HIV-1 Vif has been previously demonstrated[15] and was attributed to exposure of a nonpolar surface to the solvent. Addition of stoichiometric amounts of Cul5 inhibits zinc-induced oligomerization of HIV-1 Vif[16] suggesting that the Vif-Cul5 interface is hydrophobic. This is supported by two other studies in which mutation of hydrophobic residues in HIV-1 Vif (Ile120, Ala123, and Leu124) inhibited coimmunoprecipitation of HIV-1 Vif and Cul5.[39,40] However, these hydrophobic residues are highly conserved in Vif sequences from HIV-1, HIV-2, SIV_{Mac}, and SIV_{Agm}, and thus cannot provide an explanation for the different degrees of zinc-induced oligomerization. We aligned HIV-1 Vif sequences from the NCBI database to identify positions that are absolutely or very highly (>90%) conserved and then did the same for Vif sequences from SIV_{Agm}, HIV-2, and SIV_{Mac}. Using this approach, we identified amino acids that are highly or absolutely conserved in each family of Vif sequences, but have different polar/apolar properties (light-blue-shaded amino acids in Figure 1). For example, positions 109 and 110 in HIV-1 Vif are Leu and Tyr, respectively, while the equivalent positions in SIV_{Mac} Vif are conserved as Ser and Thr, respectively. Position 119 contains an invariant Ala residue in HIV-1 Vif, while this position is always Glu in SIV_{Mac} Vif. Position 125 in HIV-1 Vif is either Leu or Val, while it is always Arg in SIV_{Mac} Vif. Finally, position 127 in HIV-1 Vif is His or Arg, while it is conserved as Glu in the other Vif sequences. More work is required to determine whether these residues account for the observed differences in zinc-induced oligomerization and whether they are involved in Cul5 binding.

HIV-1 nucleocapsid binds zinc with picomolar (10^{-12} M) affinity.[34] This ensures that the virus can scavenge zinc ions from the host. The affinity of zinc binding to HIV-1 Vif (10^{-6} M) is several orders of magnitude weaker than nucleocapsid. However, Vif folding is not only coupled to zinc binding, but also to Cul5 binding. This is supported by the observations in this study (Figure 5) and an earlier report[16] that Cul5 recruitment by HIV-1 Vif occurs only when zinc is provided. This suggests that Cul5 can only bind to the metal-bound conformation of Vif. If true, Cul5 would increase the apparent affinity of Vif for zinc. In a study by Wolfe et al., the free energy of Cul5 binding to Vif was determined from ITC experiments to be −9.6 kcal/mol (K_d = 100 nM).[35] Thus, the free energy of zinc binding to Vif could be increased significantly in the presence of Cul5.

Recently, a report of a 3.3 Å crystal structure of HIV-1 Vif in complex with Cul5 appeared in the literature.[41] The complex also contained elongin B, elongin C, and core-binding factor subunit beta (CBF-beta), subunits of the E3 ligase complex. Vif residues I124, L125, and R127 (position 127 is histidine in our HIV-1 Vif sequence) made contacts with Cul5. I124 and L125 in Vif mediated interactions with W53 and L52 in Cul5 while R127 in Vif made ionic interactions with D55 in Cul5. Interestingly, Vif sequences from SIV_{Agm}, SIV_{Mac}, and HIV-2 contain Arg at position 125 (instead of Leu) and Glu position 127 (instead of His or Arg) (Figure 1), raising the possibility that these Vif proteins form a different molecular interface with Cul5.

Because of sequence diversity it is possible that the Vif proteins adopt folded structures that form unique interactions with Cul5. It is particularly interesting that zinc was not required for HIV-2 Vif to bind Cul5 whereas zinc was essential for Cul5 recruitment by the other Vif proteins (Figure 5). HIV-2 Vif is most closely related to SIV_{Mac} Vif; pairwise alignment reveals that the protein sequences are 79% identical and 93% similar to one another. However, zinc was required for SIV_{Mac} Vif to bind to Cul5. In the absence of zinc, the structure of HIV-2 Vif may present a minimal surface that is recognized by Cul5, allowing substantial interactions with Cul5 (Figure 6). Notably, addition of zinc did enhance Cul5 binding to HIV-2 Vif, suggesting that zinc helps to stabilize the interaction even if to a lesser degree. Fusion of Vif to MBP could also affect Vif folding. However, the requirement of zinc for the Vif-Cul5 interaction is similar regardless of whether MBP-Vif is used to pull down Cul5 (this work) or whether GST-Cul5 is used to pull down untagged Vif[16] suggesting similar *apo* and *holo* protein conformations regardless of whether the protein is tagged or untagged.

Cul5 recognition by Vif appears to involve two processes: zinc binding to the HCCH motif and stabilization of the Cul5 binding surface in Vif. Zinc binding requires orientation of the

dx.doi.org/10.1021/ic402907g | Inorg. Chem. 2014, 53, 4295−4302

ligands in the HCCH motif. In the case of HIV-1 Vif, SIV_{Agm} Vif, and SIV_{Mac} Vif, zinc binding is coupled to Cul5 binding, and in the absence of zinc the conformation that presents the Cul5 binding surface is not stable. In the case of HIV-2 Vif, the Cul5 binding surface appears to be stabilized in the absence of zinc by an unknown mechanism (i.e., zinc binding and Cul5 recognition are not coupled) (Figure 6). The zinc-bound structures of the Vif proteins encoded by HIV-1, SIV_{Agm}, SIV_{Mac}, and HIV-2 have different hydrodynamic properties as evidenced by the analytical ultracentrifugation data. This may indicate fundamental molecular differences in surfaces available for interacting with Cul5. Further studies should focus on the Vif-Cul5 interaction in the context of full length Vif. Inclusion of other binding partners to increase the Vif solubility (e.g., core-binding factor beta) might allow such an analysis to be performed. In general, our studies are consistent with the idea that zinc stabilizes a conformation of Vif that is optimized for interaction with Cul5. However, our data raise the question of whether zinc is universally critical for stabilizing the Vif-Cul5 interface.

■ ASSOCIATED CONTENT

Supporting Information

Tables of best-fit thermodynamic parameters from single-site and sequential binding models. This material is available free of charge via the Internet at http://pubs.acs.org.

■ AUTHOR INFORMATION

Corresponding Author

*E-mail: ernest.maynard@usuhs.edu.

Notes

The contents of this report are the sole responsibility of the authors and do not necessarily represent the official views of the DoD.

The authors declare no competing financial interest.

■ ACKNOWLEDGMENTS

Research was funded by grants from the Mallinckrodt Foundation and USUHS.

■ REFERENCES

(1) Hanas, J. S.; Hazuda, D. J.; Bogenhagen, D. F.; Wu, F. Y.; Wu, C. W. *J. Biol. Chem.* **1983**, *258*, 14120−14125.

(2) Berg, J. M.; Shi, Y. *Science* **1996**, *271*, 1081−1085.

(3) Brown, R. S.; Sander, C.; Argos, P. *FEBS Lett.* **1985**, *186*, 271−274.

(4) Frankel, A. D.; Berg, J. M.; Pabo, C. O. *Proc. Natl. Acad. Sci. U. S. A.* **1987**, *84*, 4841−4845.

(5) Miller, J.; McLachlan, A. D.; Klug, A. *EMBO J.* **1985**, *4*, 1609−1614.

(6) Berg, J. M.; Godwin, H. A. *Annu. Rev. Biophys. Biomol. Struct.* **1997**, *26*, 357−371.

(7) Rich, A. M.; Bombarda, E.; Schenk, A. D.; Lee, P. E.; Cox, E. H.; Spuches, A. M.; Hudson, L. D.; Kieffer, B.; Wilcox, D. E. *J. Am. Chem. Soc.* **2012**, *134*, 10405−10418.

(8) Sheehy, A. M.; Gaddis, N. C.; Choi, J. D.; Malim, M. H. *Nature* **2002**, *418*, 646−650.

(9) Conticello, S. G.; Harris, R. S.; Neuberger, M. S. *Curr. Biol.* **2003**, *13*, 2009−2013.

(10) Kobayashi, M.; Takaori-Kondo, A.; Miyauchi, Y.; Iwai, K.; Uchiyama, T. *J. Biol. Chem.* **2005**, *280*, 18573−18578.

(11) Marin, M.; Rose, K. M.; Kozak, S. L.; Kabat, D. *Nat. Med.* **2003**, *9*, 1398−1403.

(12) Mehle, A.; Strack, B.; Ancuta, P.; Zhang, C.; McPike, M.; Gabuzda, D. *J. Biol. Chem.* **2004**, *279*, 7792−7798.

(13) Stopak, K.; de Noronha, C.; Yonemoto, W.; Greene, W. C. *Mol. Cell* **2003**, *12*, 591−601.

(14) Yu, X.; Yu, Y.; Liu, B.; Luo, K.; Kong, W.; Mao, P.; Yu, X. F. *Science* **2003**, *302*, 1056−1060.

(15) Paul, I.; Cui, J.; Maynard, E. L. *Proc. Natl. Acad. Sci. U. S. A.* **2006**, *103*, 18475−18480.

(16) Giri, K.; Scott, R. A.; Maynard, E. L. *Biochemistry* **2009**, *48*, 7969−7978.

(17) Pace, C. N.; Vajdos, F.; Fee, L.; Grimsley, G.; Gray, T. *Protein Sci.* **1995**, *4*, 2411−2423.

(18) Houtman, J. C.; Brown, P. H.; Bowden, B.; Yamaguchi, H.; Appella, E.; Samelson, L. E.; Schuck, P. *Protein Sci.* **2007**, *16*, 30−42.

(19) Goldberg, R. N.; Kishore, N.; Lennen, R. M. *J. Phys. Chem. Ref. Data* **2002**, *31*, 231−370.

(20) Christensen, J. J.; Hansen, L. D.; Izatt, R. M. *Handbook of Proton Ionization Heats and Related Thermodynamic Quantities*; John Wiley and Sons, Inc.: New York, 1976.

(21) Schuck, P. *Biophys. J.* **2000**, *78*, 1606−1619.

(22) Cole, J. L.; Lary, J. W.; T, P. M.; Laue, T. M. *Methods Cell Biol.* **2008**, *84*, 143−179.

(23) Bernacchi, S.; Mercenne, G.; Tournaire, C.; Marquet, R.; Paillart, J. C. *Nucleic Acids Res.* **2011**, *39*, 2404−2415.

(24) Techtmann, S. M.; Ghirlando, R.; Kao, S.; Strebel, K.; Maynard, E. L. *Biochemistry* **2012**, *51*, 2078−2086.

(25) Yang, B.; Gao, L.; Li, L.; Lu, Z.; Fan, X.; Patel, C. A.; Pomerantz, R. J.; DuBois, G. C.; Zhang, H. *J. Biol. Chem.* **2003**, *278*, 6596−6602.

(26) Yang, S.; Sun, Y.; Zhang, H. *J. Biol. Chem.* **2001**, *276*, 4889−4893.

(27) Blasie, C. A.; Berg, J. M. *Biochemistry* **2002**, *41*, 15068−15073.

(28) Reddi, A. R.; Guzman, T. R.; Breece, R. M.; Tierney, D. L.; Gibney, B. R. *J. Am. Chem. Soc.* **2007**, *129*, 12815−12827.

(29) Gomez, J.; Freire, E. *J. Mol. Biol.* **1995**, *252*, 337−350.

(30) Grossoehme, N. E.; Akilesh, S.; Guerinot, M. L.; Wilcox, D. E. *Inorg. Chem.* **2006**, *45*, 8500−8508.

(31) Fukada, H.; Takahashi, K. *Proteins* **1998**, *33*, 159−166.

(32) Wrathall, D. P.; Izatt, R. M.; Christensen, J. J. *J. Am. Chem. Soc.* **1964**, *86*, 4779−4783.

(33) Giri, K.; Maynard, E. L. *Pept. Sci.* **2009**, *92*, 417−425.

(34) Green, L. M.; Berg, J. M. *Proc. Natl. Acad. Sci. U. S. A.* **1990**, *87*, 6403−6407.

(35) Wolfe, L. S.; Stanley, B. J.; Liu, C.; Eliason, W. K.; Xiong, Y. *J. Virol.* **2010**, *84* (14), 7135−7139.

(36) Livingstone, J. R.; Spolar, R. S.; Record, M. T., Jr. *Biochemistry* **1991**, *30*, 4237−4244.

(37) Murphy, K. P.; Xie, D.; Garcia, K. C.; Amzel, L. M.; Freire, E. *Proteins* **1993**, *15*, 113−120.

(38) Yang, A. S.; Honig, B. *J. Mol. Biol.* **1993**, *231*, 459−474.

(39) Mehle, A.; Thomas, E. R.; Rajendran, K. S.; Gabuzda, D. *J. Biol. Chem.* **2006**, *281*, 17259−17265.

(40) Xiao, Z.; Ehrlich, E.; Yu, Y.; Luo, K.; Wang, T.; Tian, C.; Yu, X. F. *Virology* **2006**, *349*, 290−299.

(41) Guo, Y.; Dong, L.; Qiu, X.; Wang, Y.; Zhang, B.; Liu, H.; Yu, Y.; Zang, Y.; Yang, M.; Huang, Z. *Nature* **2014**, *505*, 229−233.